ELSEVIER

PII: S0032-3861(97)00202-4

Polymer Vol. 38 No. 26, pp. 6363–6370, 1997

0032-3861/97/$17.00+0.00

Hard sphere behaviour of arborescent polystyrenes: viscosity and differential scanning calorimetry studies

Mario Gauthier*, Wenguang Li and Lilian Tichagwa
Institute for Polymer Research, Department of Chemistry, University of Waterloo, Waterloo, Ont., N2L 3G1, Canada
(Received 24 June 1996; revised 15 February 1997)

Two series of arborescent polystyrenes were prepared by successive cycles of functionalization and anionic grafting reactions. A target branching functionality of around 15 side chains per backbone chain and a constant branch molecular weight of either 5000 g mol^{-1} (S05 series) or 30 000 g mol^{-1} (S30 series) were used for each generation. The intrinsic viscosity of each polymer series was relatively insensitive to molecular weight, a behaviour typical of hard spheres. The S30 polymers expanded considerably in toluene relative to cyclohexane, but the S05 polymers were unaffected by change in solvent quality. Analysis by d.s.c. showed that limiting T_g values are reached in the upper generations of each polymer series, similarly to polymer networks prepared from primary chains with a low molecular weight. A lower ΔC_p and a broader transition range observed for the upper generation S05 polymers may be related to a decrease in chain mobility inside the molecules. No similar effects were observed in the S30 polymers.

(Keywords: orborescent graft polymers; branched polymers; solution properties)

INTRODUCTION

Different synthetic approaches have been suggested for the preparation of highly branched polymers, including divergent[1,2] and convergent[3,4] methods. Arborescent[5] and combburst[6] polymers also have a dendritic structure, but rely on successive grafting reactions using polymer chains rather than small molecules as building blocks. Grafting linear polystyryl anions onto a partially chloromethylated linear polystyrene yields a comb (generation $G = 0$) polymer[5]. Repetition of the chloromethylation and anionic grafting procedures leads to arborescent polymers with increasing branching functionalities, identified as generations $G = 1$, $G = 2$ and so on. The functionalization process results in random distribution of grafting sites throughout the molecule. The high branching functionalities used (typically 10–15 branches per backbone chain) also bring about a very rapid increase in the molecular weight of the polymers. Successive grafting reactions should lead to a dense, rigid core with a high segmental density, surrounded by a more diffuse, penetrable layer added in the last grafting reaction (*Figure 1*). Random distribution of the grafting sites in the chloromethylated polymer implies that the addition of side chains is not limited to the outer layer of the substrate, but can also take place in the inner portion of the molecule. In a typical grafting reaction, the molecular weight increases roughly tenfold, and the material incorporated in preceding generations accounts for less than 10% of the total mass. Excluded volume effects also limit the accessibility of grafting sites located deep inside the chloromethylated substrate. For these reasons, the chains added in a particular generation are expected to be grafted predominantly on the branches of the preceding generation, as illustrated in *Figure 1*.

The physical properties of dendritic polymers have been the topic of numerous investigations[7]. It would also be instructive to compare the physical properties of arborescent polymers with those of linear and dendritic polymers: The graft polymers can be regarded as dendritic structures where building blocks with a longer spacer length are used.

The hard-sphere behaviour of arborescent polymers in solution has been explored to some extent using light scattering[8]. In semi-dilute solutions, a stiffening of the molecular structure was observed from the comb ($G = 0$) to the next generation ($G = 1$). No significant increase in rigidity was observed from $G = 1$ to $G = 2$, however. Even for the $G = 2$ polymer, some interpenetration of the molecules was still possible, although it was clearly more limited than for linear polymers. This was thought to be a consequence of the growth mechanism postulated for the molecules, leading to a hard core–soft shell morphology.

Further to the interpenetration investigation, this paper reports on other aspects of the solution and solid state properties of arborescent polymers. The viscosity in solution, and the glass transition temperature of these materials were investigated, for comparison with the trends observed for polymers of related structure, namely dendritic, network and star-branched polymers.

* To whom correspondence should be addressed

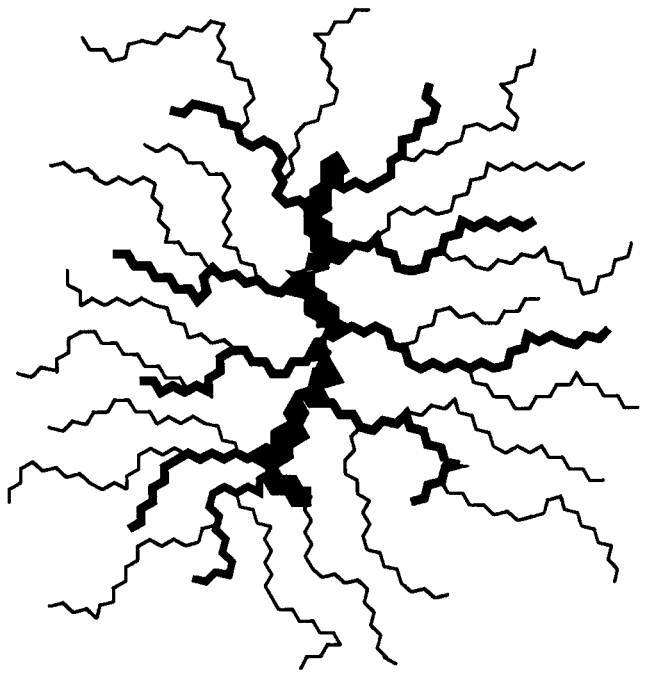

Figure 1 Simplified representation of an arborescent polymer of generation $G = 1$

EXPERIMENTAL

Materials

Details on the synthesis of arborescent polystyrenes have been reported elsewhere[5]. The two series of samples used in the measurements were prepared from a linear polystyrene core with a weight-average molecular weight $M_w = 4.8 \times 10^3\ g\,mol^{-1}$ and a polydispersity index $M_w/M_n = 1.08$. The series designated by the prefix S05 was prepared with a target branching functionality of about 15 branches per backbone chain. The branches had $M_w \approx 5 \times 10^3\ g\,mol^{-1}$ for each generation. The S30 series had a similar branching functionality, but a side chain $M_w \approx 3 \times 10^4\ g\,mol^{-1}$ for each generation. Ungrafted material was removed from the samples using precipitation fractionation in a toluene–methanol mixture. The third-generation S30 sample, because of its extremely high molecular weight, was more conveniently purified by centrifugation at 15 000 rpm from a 1% w/v tetrahydrofuran (THF) solution. The sample nomenclature identifies the series and the generation number of the polymer. For example, S05-1 refers to a $G = 1$ (twice-grafted) sample with $5 \times 10^3\ g\,mol^{-1}$ branches.

The solvents used in the viscosity and the light scattering measurements, toluene and cyclohexane (BDH, ACS reagent grade), were distilled before use.

Characterization

Static light scattering measurements served to determine the absolute weight-average molecular weight (M_w) of the graft polymers. The instrument used was a Brookhaven BI-200SM light scattering goniometer equipped with a Lexel model 95 argon ion laser operating at 514.5 nm. Stock solutions were prepared in toluene with concentrations of 0.03–10 mg ml^{-1}, depending on the sample. A series of seven solutions with equal concentration increments was prepared from the stock solution. Each solution was slowly filtered five times prior to light scattering measurements, using a PTFE membrane filter with a pore size of 0.2–2 μm, depending on the generation. Absolute molecular weights were obtained by extrapolation of the scattering data to zero concentration and angle according to the Zimm technique.

The side chains were characterized by size exclusion chromatography (s.e.c.) analysis of samples removed from the reactor before each grafting reaction. Apparent molecular weights and polydispersities were also determined for the branched polymers by the same analysis method. The equipment used was a Waters SEC system with a 500 mm Jordi DVB linear mixed-bed column and a DRI detector. Tetrahydrofuran served as the mobile phase, and the instrument was calibrated with linear polystyrene standards.

Viscosity measurements

Flow times were determined using a Cannon–Ubbelohde viscometer (capillary radius 75 μm)

Table 1 Molecular weight and branching characterization data for the arborescent graft polymers investigated. The indices br and AGP refer to the branches and to the graft polymers, respectively. The molecular weights, $(M_w)_{app}^{AGP}$, and polydispersities, $(M_w/M_n)_{app}^{AGP}$ of the graft polymers, determined by s.e.c. analysis, are apparent. All other values are absolute. The % branching densities calculated for the core portion of the molecule and for the whole molecule are identified by $(\%br)_{G-1}$ and $(\%br)_G$, respectively

S05 series								
G	$M_w^{br}/10^3$ g mol^{-1}	$(M_w/M_n)^{br}$	M_w^{AGP}/ g mol^{-1}	$(M_w)_{app}^{AGP}$ g mol^{-1}	$(M_w/M_n)_{app}^{AGP}$	f_w^{AGP}	$(\%br)_{G-1}$	$(\%br)_G$
0	4.3	1.03	6.7×10^4	4.0×10^4	1.07	14	30	2.2
1	4.6	1.03	8.7×10^5	1.3×10^5	1.07	170	29	2.2
2	4.2	1.04	1.3×10^7	3.0×10^5	1.20	2900	37	2.5
3	4.4	1.05	9×10^7	4.4×10^5	1.15	17 500	17	2.4
4	4.9	1.08	2×10^8	–	–	22 000	4.9	2.2
S30 series								
G	$M_w^{br}/10^4$ g mol^{-1}	$(M_w/M_n)^{br}$	M_w^{AGP}/ g mol^{-1}	$(M_w)_{app}^{AGP}$ g mol^{-1}	$(M_w/M_n)_{app}^{AGP}$	f_w^{AGP}	$(\%br)_{G-1}$	$(\%br)_G$
0	2.8	1.15	5.1×10^5	2.1×10^5	1.12	18	39	0.37
1	2.7	1.09	9.0×10^6	5.9×10^5	1.22	310	6.7	0.38
2	2.7	1.09	1×10^8	–	–	3400	4.3	0.39
3	2.8	1.09	5×10^8	–	–	14 300	1.9	0.38

immersed in a water bath at (25.0 ± 0.2)°C for toluene, or at (34.5 ± 0.2)°C for cyclohexane. Stock solutions of the polymers were prepared by dissolving 0.2–1.0 g of material, depending on the sample, in 25 ml distilled solvent. The maximum concentration of the solution used was adjusted to give a flow time roughly double that of the pure solvent. The solutions as well as the pure solvents were filtered through 5 μm PTFE membrane filters before the measurements. Series of five consistent (±0.05 s) flow times were obtained at seven different concentrations, using successive additions of solvent to the solution reservoir of the viscometer. The intrinsic viscosity of the polymers of each generation in the S05 and the S30 series was determined by linear extrapolation of plots of η_{sp}/c *versus* concentration c.

D.s.c. analysis

The glass transition temperature of the arborescent polystyrenes was measured with a Mettler Differential Scanning Calorimeter (d.s.c., model DSC-20) using the Mettler TA-4000 software package. The graft polymers were dried under vacuum for three days, and powdered samples of (10 ± 1) mg were sealed in aluminium pans for the measurements. Each sample was first annealed at 150°C for 5 min, quenched to 50°C and then scanned from 50 to 150°C at a rate of 20°C min^{-1}. A second run was recorded in the same temperature range, to ensure reproducibility of the results. The glass transition temperatures (T_g) reported correspond to the mid-point change in heat capacity in the transition region, and were reproducible to within ±0.5°C for successive runs.

RESULTS AND DISCUSSION

The characterization data pertaining to the two series of arborescent polystyrenes investigated are summarized in *Table 1*. The absolute weight-average molecular weight, M_w^{br} and polydispersity $(M_w/M_n)^{br}$ reported for the branches were determined by s.e.c. analysis of samples removed from the reactor prior to the grafting reaction. The polydispersity of the branches is below 1.1 in most cases, as expected from anionic polymerization techniques, indicating branches of uniform dimensions. The absolute weight-average molecular weights M_w^{AGP} reported for the graft polymers were determined from static light scattering measurements. Extrapolation on a Zimm plot to determine the molecular weight was easy, because of the good linearity of both the $\sin^2 \theta/2$ and the concentration lines. Only for sample S30-3 was significant curvature of the $\sin^2 \theta/2$ lines observed, requiring quadratic extrapolation of the data. Correspondingly, the M_w^{AGP} values given in *Table 1* are expected to be accurate within ±5–10% up to molecular weights around 10^7 g mol^{-1}, but the errors are likely larger for the higher molecular weight samples.

The apparent weight-average molecular weights $(M_w)_{app}^{AGP}$ and polydispersities $(M_w/M_n)_{app}^{AGP}$ reported for the graft polymers were determined using a linear polystyrene standards calibration curve in the s.e.c. analysis. The low values of $(M_w/M_n)_{app}^{AGP} \sim 1.1$–$1.2$ obtained in all cases are considered indicative of a narrow molecular weight distribution. Samples S05-4, S30-2 and S30-3 could not be characterized by s.e.c., because the large polymer molecules were retained in the columns by an unknown mechanism. In spite of the unavailability of s.e.c. data for some samples, comparison of the absolute molecular weights reported in *Table 1* (fourth column) shows that growth occurred uniformly for successive generations in each series. The molecular weight is expected to increase exponentially for successive grafting cycles. This seems to be the case in all but the last generations prepared. This limiting effect, also reported for dendritic molecules[1], was previously explained on steric grounds[5]. As the branching functionality of the polymers increases, grafting sites buried inside the molecule become less accessible. The grafting reaction is hindered, and fewer chains than expected are added onto the structure. Comparison of M_w^{AGP} with $(M_w)_{app}^{AGP}$ provides evidence for the compact, hard-sphere character of arborescent graft polymers. The apparent molecular weights are always lower than the absolute values determined by light scattering, a consequence of their small hydrodynamic volume resulting from branching. The difference is more pronounced for the higher generation polymers. For example $(M_w)_{app}^{AGP}$ is about 200 times smaller than M_w^{AGP} for S05-3.

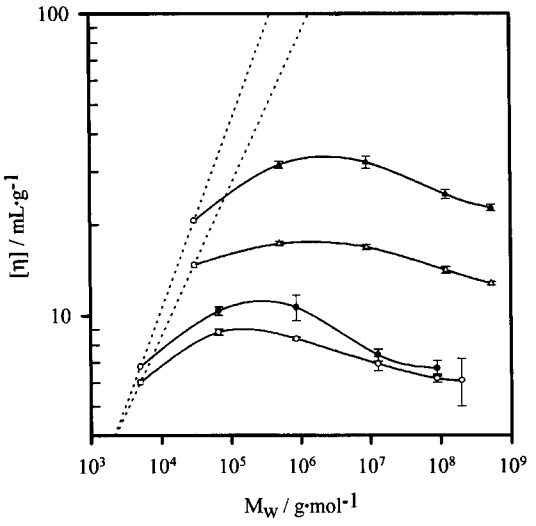

Figure 2 Intrinsic viscosities of arborescent polymers of successive generations, from the bottom to the top: S05 in cyclohexane at 34.5°C; S05 in toluene at 25°C; S30 in cyclohexane at 34.5°C; S30 in toluene at 25°C. The dotted lines show the behaviour of linear polymers

The polymers were synthesized with a target branching functionality of about 15 side chains per backbone chain for each generation. The number of branches added per molecule in a grafting reaction, reported in *Table 1*, can be calculated from

$$f_w^{AGP} = \frac{M_w^{AGP}(G) - M_w^{AGP}(G-1)}{M_w^{br}} \quad (1)$$

where $M_w^{AGP}(G)$, $M_w^{AGP}(G-1)$ and M_w^{br} are the absolute weight-average molecular weights of generation G, of the previous generation and of the side chains, respectively. The overall branching density of a dendritic polymer molecule of generation G can be expressed as the percent branching density, $(\%br)_G = 100\% \times$ (# branching units)/(# repeat units). The number of branching units in an arborescent polymer molecule of generation G is identical to the total branching functionality of the polymer, $f_w = \sum_{i=0}^{G} (f_w^{AGP})_i$. The overall branching density of the molecule is then $(\%br)_G = 100\% \times f_w/(X_w)_G$, where $(X_w)_G$ represents the weight-average degree of polymerization calculated from

the absolute weight-average molecular weight (M_w^{AGP}) of the generation G polymer. Because of the hard core, soft shell morphology postulated for arborescent polymers (*Figure 1*), it is interesting to also calculate the branching density for the core portion. The branching density of the core in a polymer of generation G can be calculated from $(\%br)_{G-1} = 100\% \times f_w/(X_w)_{G-1}$, where $(X_w)_{G-1}$ is the degree of polymerization of the preceding generation. It represents the mole fraction of branching units in the core portion of the molecule.

Viscosity measurements

Toluene and cyclohexane were selected as typical good and poor solvents for polystyrene, respectively. The intrinsic viscosities determined for the S05 and S30 polymers in each solvent are summarized in *Figure 2*. The error bars indicate the 95% confidence intervals calculated based on the propagation of variance of the individual measurements[9,10]. For each curve, the left-most point for linear polystyrene with a molecular weight of 5000 or 30 000 g mol^{-1} is followed by the corresponding arborescent polymers of generations $G = 0$, $G = 1$, etc. The data for the linear polystyrenes were calculated from published Mark–Houwink–Sakurada viscosity parameter values[11–13]. To a first approximation, all curves are relatively flat, i.e. $[\eta]$ is quite insensitive to the molecular weight of the polymers. The intrinsic viscosity of samples in the upper generations is comparable to or even slightly lower than that of the linear polymers, even though their molecular weight is up to 40 000 times larger than the linear polystyrenes. This contrasts with the behaviour of linear polymers, given by the dotted lines in *Figure 2*, with a slope of 0.5 in cyclohexane, or 0.65 in toluene.

Intrinsic viscosity, with units of ml g^{-1}, is the reciprocal of the so-called *hydrodynamic density*. This can be seen more clearly from the Einstein equation for a dispersion of hard spheres in the limit of infinite dilution

$$[\eta] = \lim_{c \to 0} \frac{\eta_{sp}}{c} = \frac{5}{2} N_A \frac{V_H}{M} = \frac{10\pi}{3} N_A \frac{R_H^3}{M} \qquad (2)$$

where N_A, V_H, R_H and M are Avogadro's number, the hydrodynamic volume, the hydrodynamic radius and the mass of the spheres, respectively. The intrinsic viscosity of the dispersion is thus determined uniquely by the density of the spheres. Globular macromolecules should have an intrinsic viscosity independent of molecular weight, as long as the ratio of mass to hydrodynamic volume (the hydrodynamic density) remains constant. Based on the results presented in *Figure 2*, arborescent polymers behave like hard spheres, to a first approximation. A more careful examination of the data reveals small variations in $[\eta]$ within each series. The variations observed are interesting in that they are clearly outside of the error limits on the individual measurements, and the trends are similar for the two series of polymers. For example, an increase in $[\eta]$ is observed from the linear to the $G = 0$ polymer (comb structure) in both the S05 and the S30 series. Monte Carlo simulations for comb polymers in solution[14] have shown that for polymers with a structure comparable to S05-0, expansion in the squared radius of gyration of the backbone by *ca.* 20% is expected. The radius of gyration of the side chains, in contrast, is essentially unaffected by branching. On this basis, the increase in $[\eta]$ (or decrease in hydrodynamic density) observed for the $G = 0$ and $G = 1$ polymers can

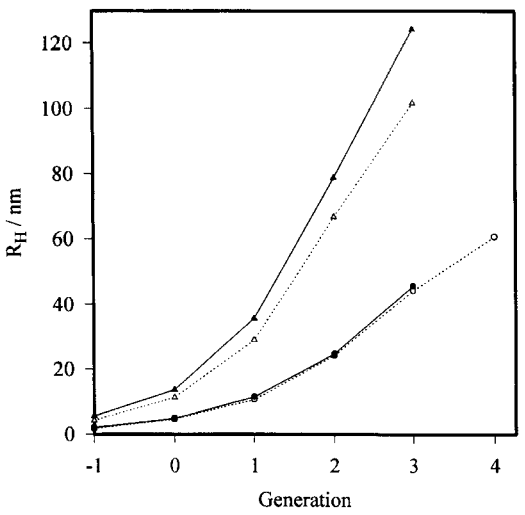

Figure 3 Hydrodynamic radii calculated from the viscosity data, from the bottom to the top: S05 in cyclohexane at 34.5°C; S05 in toluene at 25°C; S30 in cyclohexane at 34.5°C; S30 in toluene at 25°C

be attributed to backbone expansion effects analogous to those encountered in the computer simulations of comb polymers. The gradual decrease in $[\eta]$ observed both in cyclohexane and in toluene for upper generation polymers corresponds to a somewhat higher rate of increase in the mass of the molecules relative to the volume expansion, i.e. a less significant expansion of the backbone polymer.

The relatively small variation in $[\eta]$ found for arborescent polymers of successive generations are similar to the trends reported for PAMAM[15] and polyether[16] dendrimers, which display a maximum in $[\eta]$ around generations $G = 3$–5. For example, S05-0 in cyclohexane has an intrinsic viscosity about 50% higher than the upper generation and the linear polymers. This is the same relative change in $[\eta]$ observed over seven generations of tridendron polyether dendrimers prepared by the convergent growth approach. Similarly, the PAMAM dendrimers displayed a roughly two-fold variation in $[\eta]$ over eight generations. For *tert*-butoxycarbonyl-poly(α,ϵ-lysine), in contrast, Aharoni *et al.*[17] reported a constant $[\eta] = 2.5$ ml g^{-1} over 10 generations.

Variations in intrinsic viscosity are relatively minor within each series of arborescent polymers. The size of the branches, however, has a more noticeable effect (*Figure 2*), dominating $[\eta]$ and the dimensions of the molecules in solution. This is analogous to the trends reported for star-branched systems, for which $[\eta]$ correlates with the size of the arms rather than with the number of arms in the molecule[18]. The dependence of $[\eta]$ on solvent quality is also markedly different for the two series of arborescent polymers investigated. Since $[\eta]$ is inversely proportional to density, an increase in intrinsic viscosity for a polymer sample implies further expansion of the molecules. The change in $[\eta]$ in the S05 series from cyclohexane to toluene is relatively small. The S30 polymers, on the other hand, exhibit considerable expansion from a poor solvent to a good solvent, since their structure is much less crowded and rigid than the S05 polymers. The reason for the marked difference becomes obvious when comparing the overall and core branching densities reported for the S05- and S30-series polymers in *Table 1*. The branching densities

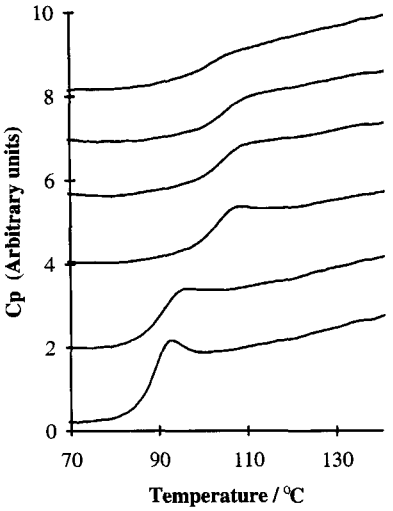

Figure 4 Thermograms obtained from the S05 polymers, linear 5000 g mol^{-1} (bottom) to S05-4 (top). The curves are shifted vertically for improved clarity

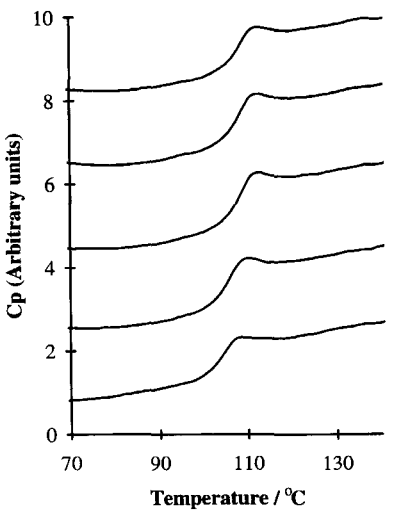

Figure 5 Thermograms obtained from the S30 polymers, linear 30 000 g mol^{-1} (bottom) to S30-3 (top). The curves are shifted vertically for improved clarity

of the S30-series polymers are about six times lower than for the S05-series.

An analogy with polymer networks, for which a lower crosslinking density leads to a greater swelling ability in good solvents, seems appropriate. The arborescent polymers could be pictured as nanonetworks incorporating randomly distributed trifunctional branching points. The effect of solvent quality on molecular expansion becomes more evident if the data in *Figure 2* are converted to hydrodynamic radii (R_H) using equation (2). The data presented in *Figure 3* show that the S05 polymers (lower two curves) display no significant expansion from a poor solvent (cyclohexane) to a good solvent (toluene), a consequence of their highly branched, rigid structure. The S30 polymers, on the other hand, have much larger radii in toluene than in cyclohexane, because of the lower branching density and the greater flexibility of the molecules. An approximately linear relationship between R_H and generation number was reported for polyether dendrimers of generation $G \geq 2$, as well as for PAMAM dendrimers of generation $G \geq 3$. The behaviour of arborescent polymers could arguably correspond to a straight line from $G = 1$ on. The transition in growth rate (the slope of the plot) to an apparently constant value also correlates with a decrease in the grafting efficiency observed for generations $G = 1$ and above[5]. The high segmental densities attained in these branched polymers were thought to result in decreased accessibility of grafting sites inside the chloromethylated substrate, and preferential reaction of sites closer to the surface. Once surface overcrowding effects become significant, growth may become determined by the number of chains which can be packed at the surface of the sphere acting as a backbone in the grafting reaction.

Differential scanning calorimetry

Traces from d.s.c. analysis of arborescent polymers in the series S05 and S30 are shown in *Figures 4* and *5*, respectively. All curves were obtained from samples of (10 ± 1) mg and are plotted on the same scale, except for vertical shifting used to improve clarity. The most obvious effect for the S05 series polymers (*Figure 4*) is a shift in T_g (the inflection point of the curves) to a higher temperature with increasing generation number up to $G = 2$. This will be discussed in more detail later. Comparison of the traces obtained for successive generations shows that the change in heat capacity is lower for the higher generation samples (upper traces) than for the $G = 0$ and $G = 1$ samples (second and third traces from the bottom, respectively). The heat capacity of polymers is related to the magnitude of vibrational and other molecular motions (e.g., pendent group rotation)[19]. The large increase in heat capacity observed in the glassy-rubbery transition temperature (T_g) region reflects the onset of crankshaft (Schatzki) motions[20] in the sample. When comparing two polymers with an identical chemical composition, a larger change in C_p is thus expected when a larger increase in chain mobility is achieved at T_g. The results presented in *Figure 4*, therefore, suggest a reduced average mobility for the polymer chains above T_g in the more crowded, upper generation samples relative to the comb ($G = 0$) polymer. The transition is also sharper for the lower- than for the upper-generation samples.

Broadening of the transition region is often observed in polymer blends and copolymers, and is generally associated with sample heterogeneity[21,22]. One could think of arborescent polymers as heterogeneous networks, with a range of crosslinking densities inside each molecule. Polystyrene chains on the outer portion of the molecule are expected to have a high mobility and a low T_g, since they are only attached to the molecule by one end. Chains in the inner portion of the molecule, on the other hand, have multiple branching points and should be much less mobile, resulting in a higher T_g. The difference in mobility between the core and surrounding chains is also reflected in the large difference in the core and overall branching densities reported in *Table 1*. The wider transition range observed for the upper generation S05 polymers may, therefore, reflect a wider range in chain mobilities in the more crowded structures.

The decrease in ΔC_p and increase in the breadth of the glassy-rubbery transition region can be easily rationalized by considering the growth mechanism of arborescent polymers. The characterization data given in

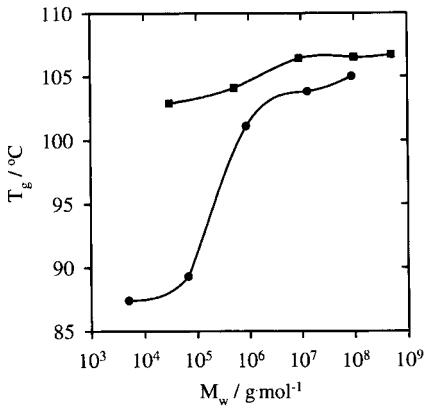

Figure 6 Glass transition temperatures determined from the mid-point of the transition range: S05 series (solid circles) and S30 series (solid squares)

Table 1 show that while M_w increases roughly by a factor of 10 for generations $G = 0$ through 2, the growth rate then decreases. From $G = 3$ to $G = 4$ in the S05 series, a relative increase in M_w of only 120% was determined. As mentioned earlier, this limited growth is attributed to overcrowding effects which decrease the accessibility of grafting sites buried inside the branched polymer structure. The outer layer of material corresponding to the last grafted generation (*Figure 1*) is rather diffuse, based on osmotic modulus measurements in semi-dilute solutions[8]. As the grafting efficiency decreases, the proportion of material contained in the mobile (outer) portion of the molecules decreases relative to the amount of less mobile core material. Consequently, the average effect measured by d.s.c. for the upper generation samples is more influenced by the core portion of the molecules.

The d.s.c. traces obtained for the S30 series polymers (*Figure 5*) are distinct from those of the S05 series. The shift in the inflection temperature (T_g) is less pronounced in this case. The change in heat capacity, as well as the breadth of the transition region are comparable for all generations. The rate of increase in M_w reported in *Table 1* for the S30 polymers is comparable to the S05 polymers, i.e. typically a 10- to 15-fold increase per generation up to $G = 2$, and a 5-fold increase from $G = 2$ to $G = 3$. The molecular weight of the branches, however, is six times higher in the S30 series than in the S05 series, resulting in a much lower branching density (*Table 1*), less crowded structure and a higher mobility for all the chains in the branched polymer. Consequently, chain immobilization effects are much less noticeable in this case, and their influence on ΔC_p is less significant than for the S05 polymers.

Glass transition temperatures of dendritic polymers have been reported for a few systems[23–25] but only two attempts[26,27] were made to correlate T_g with the structure of the polymers. Using a free volume approach, the T_g values observed for polyether dendrimers[26] were successfully correlated with the ratio of the number of chain ends to the molecular weight of the dendrimers n_e/M, according to the equation

$$T_g = T_g^\infty - K'\left[\frac{n_e}{M} - \left(\frac{n_e}{M}\right)_\infty\right] \qquad (3)$$

where $(n_e/M)_\infty$ represents an asymptotic value of n_e/M attained for high generations. The parameter T_g^∞ represents the glass transition temperature as $n_e/M \to (n_e/M)_\infty$. The ratio n_e/M is only determined by the molecular weight of the branches in arborescent polymers, and should remain constant if branches of identical size are used for successive generations. Equation (3) is not applicable to arborescent polymers, since a constant value $T_g = T_g^\infty$ would be obtained for all generations using a constant branch size (or n_e/M value). One additional problem in trying to apply equation (3) is that, in the graft polymers prepared, the molecular weight of the branches varies slightly from one generation to the next, causing fluctuations in n_e/M. The glass transition temperatures observed for the two series of arborescent polymers prepared are summarized in *Figure 6*. In all cases, T_g is lower than $T_g^\infty \approx 107.5$°C measured under the same conditions for a linear polystyrene with $M_n = 1.2 \times 10^5$ g mol^{-1}. A limiting T_g, which is higher for the S30 series than for the S05 polymers, is reached for the higher generations in each series. By far the lowest T_g values observed are for the linear and the $G = 0$ (comb) polymers. From $G = 1$ on, T_g moves closer to the limiting value. According to the free volume theory, T_g is observed when the fractional free volume in the polymer reaches a critical level $f_g \approx 0.025$. The introduction of crosslinks in a polymer 'squeezes out' free volume from the sample. Consequently, T_g is observed at a higher temperature, relative to a linear polymer, when a crosslinked sample is cooled down from the melt. Conversely, excess free volume can be introduced in the sample by incorporating more chain ends (i.e. by decreasing the molecular weight of the chains). Under these conditions, further cooling is necessary for the free volume to reach the critical value, and a decrease in T_g is observed. The preparation of a polymer network from linear chains with a relatively low molecular weight ($M_n < 5$–6×10^4 g mol^{-1} approximately, for polystyrene) makes it necessary to consider the effect of crosslinks as well as chain ends on T_g. The glass transition temperature of a network incorporating primary chains (before crosslinking) with a number-average molecular weight M_n and a crosslink density of ρ crosslinks per unit sample weight is given by

$$T_g = T_g^\infty - \frac{K_A}{M_n} + K_B\rho \qquad (4)$$

where T_g^∞ is the glass transition temperature or a high molecular weight polymer of the type used to prepare the network, and K_A and K_B are constants. The high branching functionalities attained in the upper generations may cause the arborescent polymers to behave like nanonetworks, in which a constant number of crosslinks and dangling chain ends are introduced in the system for each generation. A correlation between the branching densities reported in *Table 1* and T_g would be expected. However, no conclusive trends are observed in practice. Sample S05-4 has the lowest core branching density among the S05 series, but also the highest T_g. The variations observed in the S30-series polymers of generations 1–3 are much less significant, but the branching densities are also much lower than in the S05-series. The influence of branching density on chain mobility and T_g is, correspondingly, less pronounced.

Recently, a theoretical treatment of the glass transition temperature of networks[28] was also applied to dendrimers with some success[27]. In this case, the equation

$$T_g = [T_g^\infty - K_1(1-p)]\left(1 + K_2\frac{X_c}{1-X_c}\right) \qquad (5)$$

Table 2 Comparison of experimental glass transition temperatures and the theoretical values determined from equations (5) using $K_2 = 1.7$

S05 series		
Generation	T_g (exp)/°C	T_g (theor)/°C
−1	87	87
0	89	103
1	101	103
2	104	102
3	105	102
4	103	102
S30 series		
Generation	T_g (exp)/°C	T_g (theor)/°C
−1	103	104
0	104	107
1	106	107
2	107	106
3	107	107

was suggested where K_1 and K_2 are constants, p is the end group conversion, and X_c is the mole fraction of structural units acting as branching points. Fitting equation (5) to the experimental data was attempted, using the values $T_g^{\infty} = 370\,K$ and $K_1 = 1200\,K$[28] suggested by the authors for polystyrene and $K_2 = 0.127$[27]. Substituting $(1-p) \approx 1/X_n^{br}$ and $X_c \approx 2/X_n^{br}$, where X_n^{br} is the number-average degree of polymerization of the branches in the arborescent polymer, resulted in discrepancies of 10–30° compared with the experimental results. Fitting was also attempted using the experimental values $T_g^{\infty} = 380\,K$ and $K_1 = 840\,K$ determined from the linear polymers analysed in this work (only three samples), and treating K_2 as an adjustable parameter. The T_g values determined with $K_2 = 1.7$ compare favourably with the experimental values (*Table 2*), with the exception of the comb ($G = 0$) structures. In any case, the use of K_1 and K_2 extracted from the literature for analogous systems seems questionable, considering the distribution of branching sites inside the molecules. The situation where a significant portion of the molecule is highly mobile while the remaining material is immobilized in the core may be difficult to describe in terms of an average crosslink density X_c.

In spite of the poor quantitative agreement found between the experimental data and equation (5), it seems that the nanonetwork analogy is still the most appropriate way to describe arborescent polymers.

CONCLUSIONS

Two series of arborescent polymers were investigated using solution viscosity and d.s.c. measurements.

The intrinsic viscosity was relatively independent of the size of the molecules, a behaviour typical of hard spheres. The dimensions of the branches dominated the viscosity of the polymers, not only in terms of their influence on the dimensions of the molecules, but also their ability to expand in good solvents. The polymers with the shorter branches (S05) displayed little change in R_H from cyclohexane to toluene. The S30 polymers, however, clearly expanded in toluene.

The calorimetric measurements yielded a broad glassy–rubbery transition in the upper generation S05 samples, as well as lower changes in heat capacity relative to the linear and comb polymers. These effects were not noticeable in the S30 systems. The results obtained suggest that the mobility of the chains is reduced in at least a portion of the molecules in the upper generation S05 polymers. Theories applied to dendrimers and polymeric networks are not suitable to related experimental T_g values to the structure of arborescent polymers.

The heterogeneous character of arborescent polymers inferred from the physical characterization results presented suggests a series of experiments aimed at probing differences in chain mobility within the inner and outer portions of the molecules. Fluorescence lifetime and n.m.r. relaxation measurements have been undertaken, and will be the subject of a future report.

ACKNOWLEDGEMENTS

The financial support of the Natural Sciences and Engineering Research Council of Canada (NSERC) and of the Ontario Centre for Materials Research is gratefully acknowledged. L.T. was holder of a fellowship from the University of Zimbabwe/Canadian International Development Agency (CIDA). We are grateful to Prof. Bernard Riedl, Département des Sciences du Bois, Université Laval for giving us access to the thermal analysis equipment.

REFERENCES

1. Tomalia, D. A., Naylor, A. M. and Goddard, W. A. III, *Angew. Chem. Int. Ed. Engl.*, 1990, **29**, 138.
2. Newkome, G. R., Yao, Z., Baker, G. R. and Gupta, V. K., *J. Org. Chem.*, 1985, **50**, 2004.
3. Hawker, C. J. and Fréchet, J. M. J., *J. Am. Chem. Soc.*, 1990, **112**, 7638.
4. Miller, T. and Neenan, T. X., *Chem. Mater.*, 1990, **2**, 346.
5. Gauthier, M. and Möller, M., *Macromolecules*, 1991, **24**, 4548.
6. Tomalia, D. A., Hedstrand, D. M. and Ferritto, M. S., *Macromolecules*, 1991, **24**, 1435.
7. For representative papers on physical properties of relevance to this work, see for example (a) Hawker, C. J. and Fréchet, J. M. J., in *Step-Growth Polymers for High-Performance Materials: New Synthetic Methods*, ed. J. L. Hedrick and J. W. Labadie. ACS Symp. Ser. No. 624, American Chemical Society, Washington, DC, 1996, p. 132. (b) Voit, B. I., *Acta Polym.*, 1995, **46**, 87 (and references cited therein).
8. Gauthier, M., Möller, M. and Burchard, W., *Macromol. Symp.*, 1994, **77**, 51.
9. Reilly, P. M., van der Hoff, B. M. E. and Ziogas, M., *J. Appl. Polym. Sci.*, 1979, **24**, 2087.
10. Volk, W., *Applied Statistics for Engineers*, 2nd edn. McGraw-Hill, New York, 1969, p. 150.
11. Mukherjea, R. N. and Rempp, P., *J. Chim. Phys.*, 1959, **56**, 94.
12. Altares, T., Wyman, D. P. and Allen, V. R., *J. Polym. Sci. A*, 1964, **2**, 4533.
13. Berry, G. C., *J. Chem. Phys.*, 1967, **46**, 1338.
14. Gauger, A. and Pakula, T., *Macromolecules*, 1995, **28**, 190.
15. Tomalia, D. A., Hedstrand, D. M. and Wilson, L. R., in *Encyclopedia of Polymer Science and Engineering*, ed. J. I. Kroschwitz, Index Volume. Wiley, New York, 1990, p. 74.
16. Mourey, T. H., Turner, S. R., Rubinstein, M., Fréchet, J. M. J., Hawker, C. J. and Wooley, K. L., *Macromolecules*, 1992, **25**, 2401.
17. Aharoni, S. M., Crosby, C. R. III and Walsh, E. K., *Macromolecules*, 1982, **15**, 1093.
18. Bywater, S., *Adv. Polym. Sci.*, 1979, **30**, 89.
19. Wunderlich, B. and Baur, H., *Adv. Polym. Sci.*, 1970, **7**, 151.
20. Schatzki, T. F., *J. Polym. Sci.*, 1962, **57**, 496.

21. Nielsen, L. E., *Mechanical Properties of Polymers.* Reinhold, New York, 1962, p. 173.
22. Nielsen, L. E., *J. Am. Chem. Soc.*, 1953, **75**, 1435.
23. Miller, T. M., Nenan, T. X., Zayas, R. and Blair, H. E., *J. Am. Chem. Soc.*, 1992, **114**, 1018.
24. Miller, T. M., Kwock, E. W. and Neenan, T. X., *Macromolecules*, 1992, **25**, 3143.
25. (a) Morikawa, A., Kakimoto, M. and Imai, Y., *Macromolecules*, 1992, **25**, 3247. (b) Morikawa, A., Kakimoto, M. and Imai, Y., *Macromolecules*, 1993, **26**, 6324.
26. Wooley, K. L., Haker, C. J., Pochan, J. M. and Fréchet, J. M. J., *Macromolecules*, 1993, **26**, 1514.
27. Stutz, H., *J. Polym. Sci. B: Polym. Phys.*, 1995, **33**, 333.
28. Stutz, H., Illers, K.-H. and Mertes, J., *J. Polym. Sci. B: Polym. Phys.*, 1990, **28**, 1483.